Theory, experiment, and simulations of a symmetric arrangement of quasi-two-dimensional magnetic fluid drops

David P. Jackson*

Department of Physics and Astronomy, Dickinson College, Carlisle, PA 17013, USA

Available online 7 December 2004

Abstract

A theoretical and experimental investigation of a symmetrical arrangement of N quasi-two-dimensional magnetic fluid drops in an external field is carried out. We observe that when the distance between drops is smaller than about one drop diameter, the interactions between drops have a dramatic impact on the pattern formation process. In these circumstances, the final patterns that form are quite predictable. This predictability can be understood qualitatively by finding the rotational preference of the drops early in the evolution process using an energy minimization approach. To investigate the final state patterns, we perform a series of numerical experiments that demonstrate good agreement with the experiments.

1. Introduction

When a ferrofluid drop is placed in a Hele–Shaw cell and subjected to a perpendicular magnetic field, it undergoes a fingering instability that can lead to a complex, labyrinthine structure. The formation of these patterns has been well studied for a single-domain system but very little work has been done trying to understand multiple-domain systems. In contrast to the single-domain situation, the pattern formation process becomes very predictable. Fig. 1 shows an example of the final state patterns that can result when the interactive effects are important and when they are unimportant.

The physical system to be investigated is comprised of N equal-sized ferrofluid drops of initial radius R_0 contained in a Hele–Shaw cell consisting of two glass plates separated by a distance h. These drops are symmetrically arranged at the vertices of a regular N-sided polygon.

The magnetization M is taken to be collinear with the applied field and uniform throughout each of the domains. The magnetic (self) energy for a single domain can be written as [1]

$$E_{\text{mag}} = 2\pi M^2 V - M^2 h \oint \mathrm{d}s \oint \mathrm{d}s' \, \hat{\mathbf{t}} \cdot \hat{\mathbf{t}}' \Phi(R/h), \quad (1)$$

where V is the volume of the drop and

$$\Phi(\xi) = \sinh(1/\xi) + \xi - \sqrt{1 + \xi^2}. \quad (2)$$

Here, the integration takes place over the (two-dimensional) boundary of the domain, $R = |\mathbf{r} - \mathbf{r}'|$ is the

---

*Corresponding author. Tel.: +1 717 245 1073;
fax: +1 717 245 1642.

E-mail address: jacksond@dickinson.edu (D.P. Jackson).
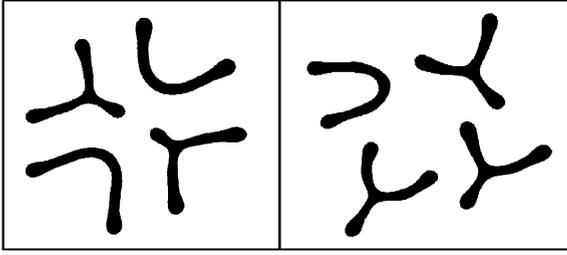
Fig. 1. Experimental final state patterns when interactions play an important role (left) and when they are insignificant (right).

distance between two points on the contour, and $\hat{\mathbf{t}}$ and $\hat{\mathbf{t}}'$ are unit tangent vectors at these points.

When considering a multi-domain system, each drop will contribute this self-energy but there will also be interaction terms of the form

$$E_{ij} = -M^2 h \oint \mathrm{d}s_i \oint \mathrm{d}s_j \hat{\mathbf{t}}_i \cdot \hat{\mathbf{t}}_j \Phi(R_{ij}/h), \qquad (3)$$

where the subscripts now refer to contours on separate domains. Because we are only interested in how the interactions influence the pattern formation process, we focus our attention on the total interaction energy of the system, given by

$$E_{\mathrm{int}} = \frac{1}{2} \sum_{i \neq j} E_{ij} = \sum_{i<j} E_{ij}. \qquad (4)$$

2. Energetically preferred rotational states

We are interested in finding the preferred energy states for this system early in the evolution. Thus, we introduce pure mode disturbances of the form $\varsigma_i \cos[n_i(\theta + \alpha_{ij})]$, where the mode number n_i indicates the number of bumps on domain i, and α_{ij} is the rotation angle of drop i with respect to drop j. Linearizing the interaction energy with respect to the small parameter ς_i/R_0 then gives [2]

$$E_{ij} = I_{ij}^{(0)} + \varsigma_i A_{ij} \cos n_i \alpha_{ij} + \varsigma_j A_{ji} \cos n_j \alpha_{ji} \qquad (5)$$

where $I_{ij}^{(0)}$ is the interaction energy for two circular domains and A_{ij} is the *amplitude coefficient* that depends on the mode number of the ith drop (n_i) and the distance between drops i and j.

Symmetry dictates that we can, without loss of generality, focus our attention on a single domain (say, drop 1). Incorporating only that portion of the interaction energy that depends on drop 1 and writing the rotation angles as $\alpha_{ij} = \alpha_{12} + (j-2)\pi/N$, we find an expression for the extreme angles α_{12}^* that involves complicated summations involving the amplitude coefficients. However, since the interactions do not play a significant role when the drops are separated by more

than about one drop diameter, it is only the two nearest neighbors that will affect any particular drop. By including only nearest-neighbor interactions and using the fact that $A_{12} = A_{1N}$, we find the following expression for the extreme angles:

$$\tan n_1 \alpha_{12}^* = -\frac{\sin[(N-2)n_1\pi/N]}{1 + \cos[(N-2)n_1\pi/N]}, \qquad (6)$$

valid as long as the denominator is nonzero.

To guarantee we have an energetic minimum, we require the second derivative of the energy (evaluated at α_{12}^*) to be positive. This allows us to write the minimum energy rotational states for drop 1 as

$$\alpha_{12}^* = -\frac{N-2}{2N}\pi + \frac{l\pi}{n_1}, \qquad (7)$$

where l is an integer that satisfies

$$2l + 1 < \frac{N-2}{N}n_1 < 2l + 3. \qquad (8)$$

Thus, to determine the preferred orientation of our system of drops, we first calculate l using Eq. (8) and then determine the preferred angle of drop 1 from Eq. (7). The orientation of the other domains can be obtained by a similar procedure. In our case, since we assume all of the drops begin with the same initial radius, it is likely (see Ref. [3]) that all of the drops will have the same initial perturbation. Thus, for the remainder of this paper, we will assume that all drops have the same mode number n.

As an example, suppose we have a configuration with $N = 3$ and $n = 2$. We then find that $l = -1$ which yields $\alpha_{12}^* = -2\pi/3$. The preferred angles for the other two drops are then easily obtained by symmetry. Fig. 2 shows the theoretical predictions and the experimental results for three different configurations. The agreement between theory and experiment is quite good.
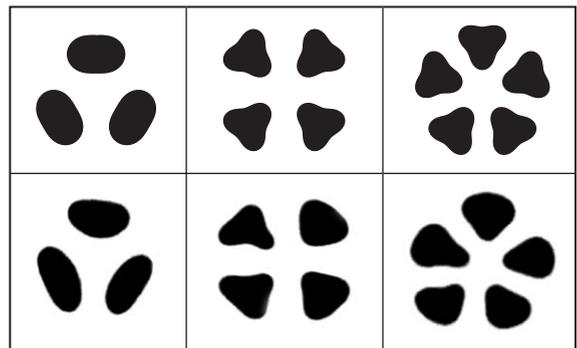
Fig. 2. Theoretical preferred states (top) and experimental realizations (bottom) for three different configurations.

3. Symmetric configurations

The results presented in Fig. 2 are ultimately based on Eq. (6), and as previously noted, this equation is only valid when the denominator is nonzero. This results in a constraint between the number of drops N and the mode number n, namely

$$\frac{N-2}{N}n \neq 2k+1, \quad \text{where } k = 0, 1, 2 \dots. \tag{9}$$

By calculating the nearest-neighbor interaction energy, one can show that these mode numbers lead to an interaction energy that is independent of rotation angle. Thus, there is no minimum (or maximum) for these special values.

This curious situation can be understood as a geometric symmetry between the angle formed by nearest-neighbors ($\pi - 2\pi/N$) and the angle formed by a protrusion and an indentation on a single drop (π/n). When these two angles are equal, we get precisely the condition disallowed by Eq. (9) resulting in an interaction energy that is independent of drop rotation. Table 1 give a partial list of configurations that have this symmetry condition and therefore do not have an orientational preference as predicted by this analysis. (It is interesting to note that there are *no* symmetric configurations for systems in which the number of drops is given by $N = 2(2m-1)$, where m is a positive integer.)

4. Computational and experimental results

To study this system far into the nonlinear regime requires a computational approach. Beginning with the Navier–Stokes equation for a viscous magnetic liquid, we use the standard Hele–Shaw approximations that lead to a two-dimensional velocity field given by Darcy's law

$$\mathbf{v} = -\frac{h^2}{12\eta}\nabla\Pi, \tag{10}$$

where η is the viscosity of the ferrofluid and Π is a generalized pressure that includes the magnetic effects. We assume the outer fluid has a negligible viscosity and take the pressure outside the ferrofluid to be constant.

The incompressibility condition then leads to solving Laplace's equation within the interior of the ferrofluid domain with boundary condition given by the generalized pressure at the interface. The evolution equation is then obtained using a conformal mapping algorithm for solving a Dirichlet problem on an arbitrarily shaped domain [4,5].

Extending this technique to a multi-domain system is relatively straightforward if we continue to assume a constant pressure outside the ferrofluid domains. We note that this approach renders the domains hydrodynamically isolated from each other. That is, any interactive effects are due solely to the magnetic interactions. This should be a good approximation if the ferrofluid is surrounded by air.

In our experiments, the plate spacing is approximately 1 mm and the droplet diameters are about 2 mm. The ferrofluid is surrounded by a water/tween mixture to help minimize sticking with the glass plates and the magnetic field was quickly ramped up to a final field value of about 200 G.

Fig. 3 shows a comparison between computational and experimental evolutions for a system consisting of

Table 1
A partial list of N and n values that give rise to special symmetric configurations with no rotational preference

N	3	4	5	7	8	$\cdots$
	3	2	5	7	4	$\cdots$
n	9	6	15	21	12	$\cdots$
	15	10	25	35	20	$\cdots$
	$\vdots$	$\vdots$	$\vdots$	$\vdots$	$\vdots$	$\ddots$
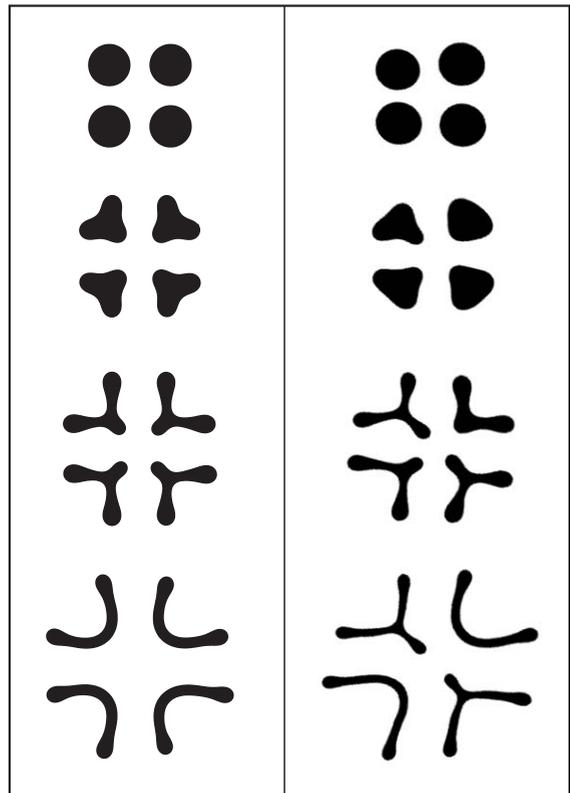
Fig. 3. Numerical evolution (left) and experimental evolution (right) for a system of four ferrofluid drops. Time runs downward.

four ferrofluid drops. Experimentally, it was difficult to obtain four equal-sized drops and to arrange them in a perfectly symmetric manner. Nevertheless, the numerical solutions show remarkably good agreement with the experimental results (see also Ref. [6]).

One noticeable difference that can be seen in Fig. 3 is that only two of the drops in the experiment have lost their center-pointing finger whereas all four drops lose this finger in the simulations. We believe this is due to sticking with the glass plates in the experiment. We can simulate this effect in the simulations simply by terminating the evolution when the velocity of droplets decreases to some arbitrary value. We also note that the finger width in the final state of the simulation is thicker than in the experiment. This is simply because the final magnetic field value used in the simulation was slightly lower than that used in the experiment.

Acknowledgments

References

[1] S.A. Langer, R.E. Goldstein, D.P. Jackson, Phys. Rev. A 46 (1992) 4894.
[2] D.P. Jackson, B. Gantner, Phys. Rev. E 64 (2001) 056230.
[3] A.J. Dickstein, et al., Science 261 (1993) 1012.
[4] D. Bensimon, et al., Rev. Mod. Phys. 58 (1986) 977.
[5] D.P. Jackson, R.E. Goldstein, A.O. Cebers, Phys. Rev. E 50 (1994) 298.
[6] D.P. Jackson, Phys. Rev. E 68 (2003) 035301(R).